Remote Sensing of Environment 286 (2023) 113427

Contents lists available at ScienceDirect

Remote Sensing of Environment

journal homepage: www.elsevier.com/locate/rse

Thermal unmanned aerial vehicles for the identification of microclimatic refugia in topographically complex areas

Raúl Hoffrén [a,*], María B. García [b]

[a] Geoforest-IUCA, Department of Geography and Land Management, University of Zaragoza, Pedro Cerbuna 12, 50009 Zaragoza, (Spain)
[b] Pyrenean Institute of Ecology, Spanish National Research Council (IPE-CSIC), Av Montañana 1005, 50059 Zaragoza, (Spain)

ARTICLE INFO

Edited by Dr. Marie Weiss

Keywords:
UAV
Thermal infrared
Mountain areas
Gradient boosted models
Biodiversity conservation

ABSTRACT

Biodiversity loss is one of the most relevant consequences of climate change. Therefore, identifying areas and environmental features that allow certain organisms to be less exposed to the effects of the current global warming is priority for biodiversity conservation. In this study, we describe a novel approach for the identification of microclimatic refugia in rugged mountain areas, specifically for the detection of most thermally stable areas, using an unmanned aerial vehicle (UAV) capable of recording in the visible and thermal infrared spectral bands. We estimated land surface temperatures (LST) at very-high spatial resolution in six topographically complex sectors of the Pyrenees (NE Spain), across seasons with vegetative activity (summer 2020, autumn 2020, spring 2021, and summer 2021), and at two thermally contrasted times of the day (early in the morning: LST_{min}, and in the afternoon: LST_{max}). LST were validated with a network of miniaturized temperature sensors in the field. LST_{min} and LST_{max} allowed us to calculate the daily thermal range of each sector across the seasons, and thus the most thermally stable areas over the year. To reveal the importance of different variables on low and narrow thermal ranges we applied Gradient Boosted Models to seven terrain variables derived from ALS-LiDAR (slope, northness, eastness, heat load, wind exposure index, SAGA's topographic wetness index, and vector ruggedness measure) and a proxy of forest density through the three-dimensional point clouds of the UAV data. The northness was the variable that most promoted thermal stability, followed by the slope and forest density, so that microclimatic refugia resulted to be located in northern slopes, small sites under rocky cliffs, and forested areas. Our results demonstrate that thermal UAVs can become promising tools for the identification of microclimatic refugia in topographically complex areas, providing information at unprecedented spatial resolution, and thus of high interest for biodiversity conservation.

1. Introduction

Climate is one of the most important determinants of species distribution, and many studies have demonstrated the critical role of climate change on the structure and composition of communities, habitats and ecosystems (Ashcroft and Gollan, 2013; Chen et al., 2011; Choler, 2017; Pauli et al., 2012; Pugnaire et al., 2019). In the highly diverse and environmentally heterogeneous mountain regions, climate is modulated by the altitudinal gradient, topography and land cover (Körner, 2004). Roughness contributes to the diversity of fine-scale landforms, transforming the regional climate into a variety of local microclimates over short distances (Ackerly et al., 2010; Hoffrén et al., 2022). In addition, forests dramatically buffer extreme climatic conditions for understory organisms (De Frenne et al., 2021; Greiser et al., 2019). Thus, mountain ranges often constitute mosaics of microclimates, some of which can act as microclimatic refugia (thereafter, microrefugia): small patches buffered from contemporary climate change because of their lower exposure to extreme temperatures and external fluctuations (Keppel et al., 2017). Their stable climatic conditions result from the modification of regional climate, so that local climate is decoupled from the general due basically to the effect of topography and the shade provided by forests (Ashcroft et al., 2012; Dobrowski, 2011; Keppel et al., 2015). Identifying and protecting microrefugia is a priority for biodiversity conservation, as they give species the opportunity to persist when they are not capable of adapting or migrating in climate change scenarios (Graae et al., 2018; Hylander et al., 2015; Keppel et al., 2015; Suggitt et al., 2018), constituting the last citadel for their survival (Collins et al., 2013; García et al., 2020; Wilson et al., 2019) and providing resilience to landscapes

* Corresponding author.
E-mail addresses: rhoffren@unizar.es (R. Hoffrén), mariab@ipe.csic.es (M.B. García).

https://doi.org/10.1016/j.rse.2022.113427
Received 10 June 2022; Received in revised form 16 December 2022; Accepted 22 December 2022
Available online 29 December 2022

(Andrew and Warrener, 2017).

Until now, most studies focused on detecting microrefugia have used fine-scale topoclimatic models derived from topographic and forest variables, and microclimatic data (e.g., Ashcroft et al., 2012; Greiser et al., 2018; Maclean et al., 2016; Meineri and Hylander, 2016). Topography and vegetation variables have usually been generated using Light Detection and Ranging (LiDAR) technology, which makes it possible to represent different terrain attributes by creating Digital Terrain Models (DTMs) at high spatial resolution. Due to the ability of LiDAR signals to penetrate the canopy, it is also possible to model the horizontal and vertical structure of vegetation, such as canopy height, density, or their variability. Regarding microclimatic information, previous studies have commonly used meteorological stations, miniaturized field sensors and thermal cameras. The former often at regional or national scales (e.g., Niskanen et al., 2017; Suggitt et al., 2018), while mini-sensors are frequently used in smaller and topographically complex areas (e.g.; Davis et al., 2019; Macek et al., 2019; Williamson et al., 2021). There has been an increasing interest in using mini-sensors in the last decade because meteorological stations cannot accurately predict organismal responses to climate change, as they are very sparse in the territory and measure in open areas at 1.5–2 m height above ground (Zellweger et al., 2019). The advantage of mini-sensors lies in that they can be placed in many locations and at ground level, where most organisms live (Ashcroft et al., 2009; Dobrowski, 2011; Greiser et al., 2019; Lembrechts et al., 2020). However, both meteorological stations and mini-sensors provide spatially discrete point-based measurements, and make further processing necessary to interpolate temperatures (Zellweger et al., 2019). In addition, mini-sensors deployment, maintenance, and data download are highly time-consuming, limiting their distribution over wide areas.

Remote sensing can help overcome these limitations, specifically thermal infrared (TIR) sensors, as they offer opportunities to produce detailed and spatially continuous data of land surface temperatures. Nevertheless, very few studies have used TIR sensors to identify microrefugia successfully. Spaceborne sensors, such as MODIS (e.g., Mackey et al., 2012) or Landsat (e.g., Andrew and Warrener, 2017), offer a wide spatial coverage and accurate temporal resolutions, but all of them fail when it comes to identifying temperatures at high spatial resolution. Manual thermo-cameras are a good option to capture fine-scale temperatures in a specific location during different times of the day or over the year. For instance, García et al. (2020) used TIR imagery from a thermo-camera in two rocky cliffs sectors of the Spanish Pyrenees to investigate the thermal profile and stability of two populations of relict and endemic plant species. However, the images these cameras take are limited by the spatial coverage available from the shooting place and its accessibility. These constraints can be solved by using TIR sensors on board unmanned aerial vehicles (UAVs), thanks to their great mobility and the capability of recording land surface temperatures at centimetric resolution (Faye et al., 2016; Zellweger et al., 2019). In addition, UAVs allow deriving high-dense tridimensional point-clouds from very-high resolution overlapping images (Puliti et al., 2015) through *Structure-From-Motion* (SFM) algorithms (Remondino et al., 2014) based on traditional photogrammetric techniques (Messinger et al., 2016), which are very useful to reproduce several features of the territory. To the best of our knowledge, the use of thermal sensors attached on UAVs to detect microclimates and thermal refugia remains rather unexplored, and there is only one antecedent developed by Milling et al. (2018), which used a thermal UAV in the Lemhi Valley of east-central Idaho (USA), dominated by dense clusters of shrubs and mounded micro-topography, to identify refugia for ground-dwelling animals.

In this study, we aim to demonstrate the suitability of thermal UAVs for identifying thermal stable areas in topographically complex mountain regions. This approach could allow the detection of microrefugia for very many and most abundant small plants and animals in an easy and unprecedented precise way. We assume that stability emerges as a result of decoupling between near-ground local and regional temperatures due to different factors (Dobrowski, 2011; Hoffrén et al., 2022), and adapt the method used by García et al. (2020) of considering areas of narrowest thermal range within a spatial matrix as microrefugia. For that purpose, we will generate thermal landscapes at a very-high spatial resolution in very contrasted moments of the day across seasons and, after validating temperatures provided by TIR imageries with a set of miniaturized temperature sensors, we will identify which environmental factors promote stability. We establish two main hypotheses: (1) UAVs can be used in a reliable way to produce highly accurate thermal landscapes at centimetric scale from estimated land surface temperatures, and (2) by overlapping multi-temporal layers of land surface temperatures and combining them with terrain variables it is possible to identify the most thermally stable areas and variables that promote microrefugia for biodiversity.

2. Materials and methods

2.1. Study area

The study was conducted in a region of high biodiversity of southern Europe: The Ordesa and Monte Perdido National Park (thereafter, PNOMP), in the South part of the Central Pyrenees (Fig. 1) (42.6456°N, 0.0361°E). It contains almost 1400 vascular plants, around 10% of the European flora in just 30 ha (Pardo et al., 2017). Specifically, we focused on two areas located at similar altitude (2100–2200 m a.s.l.) in Ordesa and Pineta valleys, in the ecotone between the forest and the alpine grassland, characterized by high roughness, with steep slopes and contrasted expositions that vary at fine scale. Each area consisted of three study sectors separated by 1000–1500 m in the Ordesa area and about 50 m in the Pineta area. Sectors were selected for their environmental heterogeneity, often with small stands of black pine forests (*Pinus uncinata* Mill.), and open areas with different abundance of vegetation and rocks: from dense grasslands till screes, short cliffs and rocky outcrops.

Study sectors O1 (42.6378°N, 0.0593°W), O2 (42.6325°N, 0.0408°W) and O3 (42.6292°N, 0.0270°W) were located in *Sierra de las Cutas*, on top of the Ordesa Valley (Fig. 1). This is a *E*-W oriented convex area characterized by the presence of steep slopes in the northern part, which descends towards the bottom of the valley, and a gentler slope in the south part, where subalpine grasslands are mixed with rocky outcrops and black pine forest stands. O1 is formed by two opposite slopes oriented to the south and to the north, both consisting of grassland mixed with small rocky outcrops, although black pine forests and larger rocky cliffs can be found in the north-facing slope. O2 is mainly a sunny slope with a mixture of grassland, rocky outcrops and black pine forest in its lower part, and a small sector of the north-facing slope with trees and screes. O3 is characterized by a prominent north-facing cliff with large rocky outcrops and a small plain at the top that becomes a gentle south-facing grassland slope.

Study sectors P1 (42.6779°N, 0.1147°E), P2 (42.6760°N, 0.1180°E), and P3 (42.6745°N, 0.1215°E) were located in *Sierra de Espierba* in the Pineta Valley (Fig. 1). The bottom part of this small E-W oriented hanging valley dominated by subalpine grasslands that continue towards the south-faced slope, whereas the north-faced slope is very steep and made of large limestone rocks dominated by black pine open forests. In addition, small patches of bare soil, screes and rocky outcrops can be found. In the eastern part (P3), the steep north-faced slope transforms into a large scree with some outcrops of limestone rock and scattered patches of pine groves of black pine. In the western part of the sector (P1, P2), the south-faced slope is covered by a mix of subalpine shrublands, screes, and black pine forests.

2.2. UAV thermal data acquisition and processing

To estimate land surface temperatures (LST), we used a Parrot *Anafi Thermal*, a multirotor UAV equipped with both TIR and high-resolution

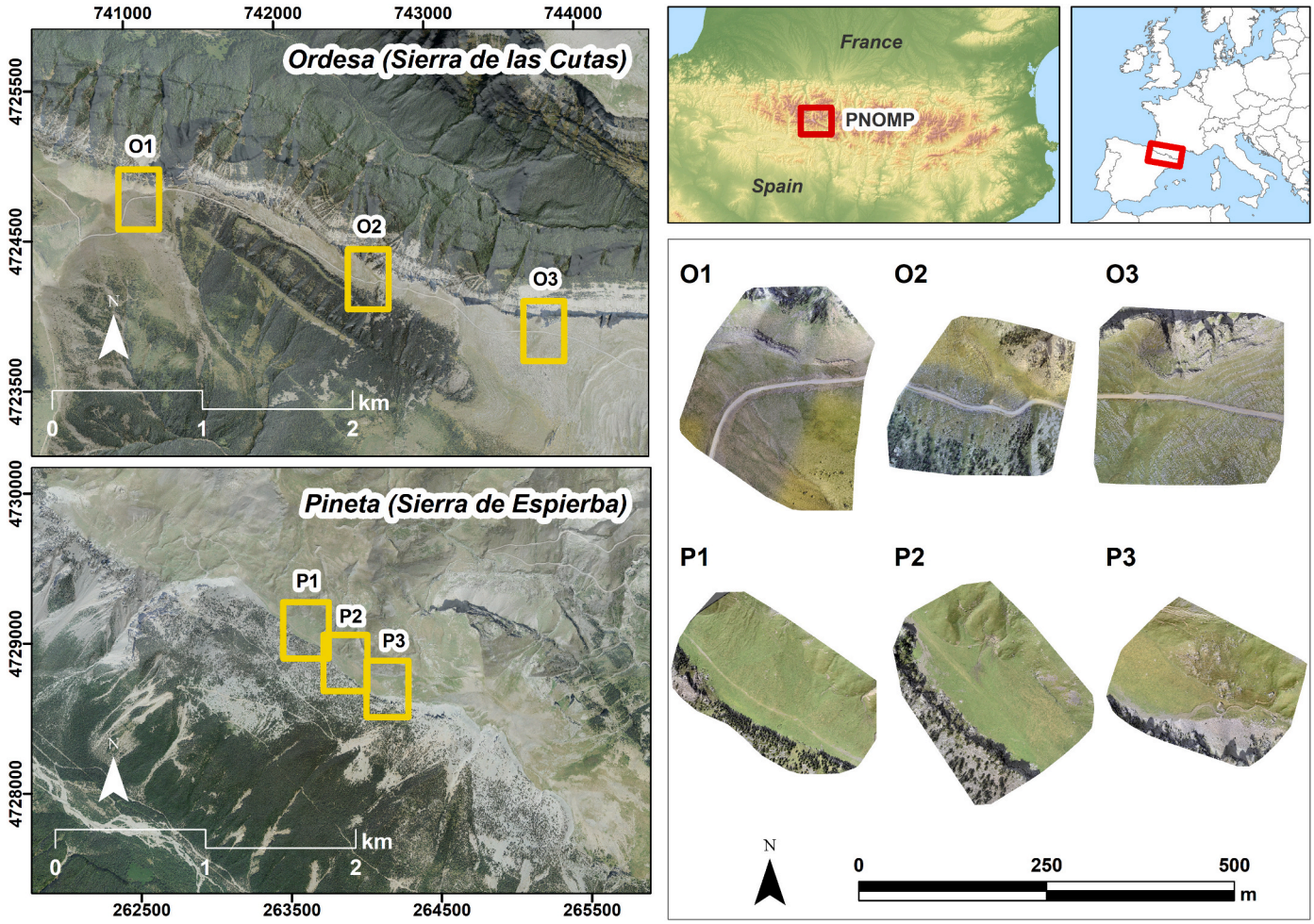

Fig. 1. Study area on the south side of the Central Pyrenees: The Ordesa and Monte Perdido National Park (PNOMP), and the six sectors where the UAV flight campaigns were conducted: on Jul 31, 2020; Oct 31, 2020; May 17, 2021; and Aug 15, 2021 in the Ordesa sector; and on Aug 1, 2020; Oct 30, 2020; May 18, 2021; and Aug 13, 2021 in the Pineta sector.

RGB cameras that work together. The former is a FLIR Lepton 3.5 radiometric sensor with 160 x 120px resolution, which allows the estimation of LST from the TIR region, located between 8 and 14 μm. This radiometric sensor is factory calibrated and, according to the manufacturer, its calibration must not be carried out unless necessary (i.e., after a crash).

In order to determine the spatial variability of temperatures over a year, we made 4 UAV flight campaigns in the six study sectors: summer 2020, autumn 2020, spring 2021, and again in summer 2021. Winter was not of interest for this study due to the snow covering both sectors. In both summer flights, we chose the hottest days of the season to better capture maximum extreme temperatures. To estimate daily thermal stability, in each campaign we made 2 flights: one early in the morning (6–8 a.m. UTC) to record the daily minimum temperature, and another in the afternoon (2–4 p.m. UTC) to record the daily maximum temperature. Thus, the number of flights made by season was 12, reaching a total of 48 flights for all campaigns. All these flights allowed us to estimate daily and across-seasons thermal ranges. The UAV flew at 80 m from the ground to obtain LST data at 3 cm/px spatial resolution. We established a nadiral incidence angle (90°), an overlap between photographs of 80% and 70% along and across track, respectively, and a 0.95 nominal emissivity value. The duration of each flight was about 20 min and all of them were automated using *PIX4Dcapture* software. A visual depiction of a typical UAV survey can be seen in Fig. S1 of Supplementary Materials.

We processed TIR data to generate thermal landscapes using *PIX4Dmapper* software. For this, we generated thermal rasters of the daily minimum temperatures (LST_{min}) and the daily maximum temperatures (LST_{max}) for each area and campaign. From them, we calculated the Daily Thermal Range (DTR) as the difference between LST_{max} and LST_{min}, and the Mean Thermal Range (MTR), as the average DTR over the three different seasons (autumn 2020, spring 2021, and the mean DTR of summer 2020 and 2021). MTR allowed us to identify the areas that proved to be most thermally stable across the three seasons (narrowest ranges), which corresponded to the lowest values of the distribution. We then extracted pixels of lowest MTR values located below deciles 1, 2, and 3 of the frequency distribution, to which we referred as of very-high thermal stability (D1), high thermal stability (D2), and medium-high thermal stability (D3), respectively.

2.3. Accuracy assessment of UAV-LST data

To validate the UAV-LST data, before the first flight we deployed 21 miniaturized field sensors across the heterogeneous landscape (open and forested areas) of the six study areas. They were Maxim Integrated's iButtons dataloggers, successfully used in several studies about microclimates (e.g., Ashcroft et al., 2012; Ashcroft and Gollan, 2013; Lembrechts et al., 2020; Maclean et al., 2016; Williamson et al., 2021). All of them were scheduled to collect temperatures every hour, and buried at ~5 cm below surface to protect them from heavy solar insolation after being sheltered inside a small plastic container to avoid moisture concentrations that could short-circuit them. The spatial location of each

iButton was recorded with a Garmin eTrex® 20 GPS. To avoid the mean geolocation error of the GPS, which was not of sub-meter accuracy, sensors were placed in easy identifiable locations for subsequent correction in the office using the very-high resolution RGB images taken by the UAV. Temperatures recorded by iButtons during each of the UAV flights were confronted with the temperatures provided by thermal rasters in the placement of iButtons (Pearson correlation of linear regression). To account for the positioning error of non-differential GPS (Piedallu and Gégout, 2005), we confronted three temperature values: the one corresponding to the pixel of the iButton placement, and averaged pixel values within 2 and 15 m buffer radius around it. The accuracy of UAV-LST data was then assessed by computing the coefficient of determination (r^2) and the root-mean-square error (RMSE), and the larger buffer resulted in slightly higher r^2 and lower RMSE. Correlations were estimated for different sets of temperature records: pooling all campaigns, study sectors, for the two habitats (open vs. forest), and also separately.

In addition, since iButtons were placed below ground, and the thermal camera of the UAV records temperatures on the surface and at the level of tree canopies, we conducted an additional UAV flight of validation in the Pineta Valley sector, over an homogeneous southern slope composed of patches of subalpine grasslands, screes, and black pine forests. We deployed 10 TOMST's Temperature-Moisture-Sensor (TMS) dataloggers (Wild et al., 2019) in the flight area, following the same method as with the iButtons. TMS dataloggers are capable of recording temperatures at the same point from three sensors covered by a little hat (8 cm below ground, 2 cm on the ground, and at 15 cm above ground), being 5 of them in open habitats and 5 within forest. The flight was performed in summer 2021 in the maximum daily heat moment (~2 p.m. UTC) using the same flight parameters applied in previous campaigns. The correlation between UAV-LST and TMS sensors allowed us to test how well they matched, at ground level or below ground, both in open and forested areas, and thus if records at the canopy level constitute a good proxy for the forest interior. In this case, the correlation resulted to be best for the 2 m radius buffer, given that open and forest patches are small and the buffer of 15 m radius often invades part of the opposite patch to the analyzed.

2.4. Terrain variables acquisition

To identify the environmental factors that contribute to the occurrence of the thermally stable areas, we modeled the effect of eight variables in the six study areas on MTR. Variables were derived from two sources: i) public ALS-LiDAR data of the Spanish National Plan for Aerial Orthophotography project (PNOA), for slope, aspect (northness and eastness components), heat load, wind exposure index (WEI), SAGA's topographic wetness index (SWI), and vector ruggedness measure (VRM); and ii) the high-dense classified 3D point-clouds of the UAV-RGB data, for the proxy of forest density or canopy forest. Although elevation is a key variable in the modification of temperatures in mountainous areas, it was not of interest in this case because surveyed areas have little differences in elevation. Our design, thus, allows that the importance of terrain variables for producing microclimates emerge.

ALS-LiDAR flights in PNOMP were conducted in 2010. The sensor operated at a wavelength of 1064 μm with a scan angle of ±29° from the nadir. The average point-cloud density was 1.5 point/m^2 and all returns had a vertical accuracy better than 0.2 m. We removed noise and overlapping returns and then ground points were classified using MCC 2.1 command-line tool (Evans and Hudak, 2007) and interpolated with a point-TIN-Raster interpolation method (Renslow, 2013) to generate a Digital Terrain Model (DTM) of 1 m grid resolution following Montealegre et al. (2015). From the DTM we generated the slope (in degrees) and the aspect (in radians) using the "raster" package for the R environment (Hijmans, 2021). The latter was split into the northness and the eastness, as the cosine and sine of the aspect, respectively, to transform the circular component of the variable into continuous, which ranged between −1 (south or west) and 1 (north or east). We also used the "Terrain Analysis" module implemented in SAGA-GIS (Conrad et al., 2015) to generate the rest of the LiDAR-based variables: heat load, as a proxy of solar exposure; WEI and SWI, as proxies of potential areas of cold-air drainage; and VRM, as a measure of the topographic heterogeneity and roughness. For generating the heat load, we chose an "Alpha max" (amax) value of 202.5°. For WEI, we applied a maximum search distance of 300 km, an angular step size of 15°, and an acceleration of 1.5, avoiding constant wind direction and without averaging elevation. For calculating SWI, we used the tool SAGA Wetness Index, which is based on the Topographic Wetness Index (TWI) (Beven and Kirkby, 1979) but provides more accurate topographic moisture predictions in cells located in concave areas by not treating run-off as a thin film of water (Böhner et al., 2002; Böhner and Selige, 2006). Thus, SWI predicts a more realistic and higher potential soil moisture in concave areas with a small vertical distance to a channel compared to TWI (Olaya and Conrad, 2009). Hedley et al. (2013) found SWI more sensitive to the impacts of small vertical distances on soil moisture than TWI, thus being more appropriate for detailed studies. We applied the following parameters for SWI calculation: an average suction value of 10, the square root of the total catchment area, a catchment slope, a minimum slope value of 0, an offset slope value of 0.1, and a slope weighting factor of 1. Lastly, for VRM we used a 3 × 3 cells circular radius without distance weighting.

RGB images captured by the UAV were used to generate high-dense tridimensional point-clouds through SFM photogrammetric techniques implemented in *PIX4Dmapper* software. Point-clouds had an average nominal density of 950 points/m^2 for the whole areas and were automatically classified according to the main land cover in the same LiDAR point-clouds default categories. By visual analysis, a few points of low vegetation (shrublands) that had been classified as ground were reclassified. Point-clouds were then filtered out by the three vegetation categories (low, medium, and high vegetation). Finally, we used the tool "LAS Points Statistics as Raster" in ArcMap v.10.7.1 to calculate the proportion of vegetation returns (in %) of the total returns in each pixel as a proxy to identify forest density, defined as the number of vegetation returns divided by the total number of returns within each pixel of a 1 m spatial resolution raster.

2.5. Relevant variables for microrefugia: combining thermal landscapes and terrain features

Terrain variables acquired in raster format were stacked together along with the MTR stability raster. As the latter had higher resolution than the terrain variables, it was resampled to a spatial resolution of 1 m/px by cubic convolution, which calculated the value of each pixel by fitting a smooth curve based on the surrounding 16 pixels. To identify which factors have more effect on the stability (low MTR), we randomly sampled 500 points in each of the six areas of flight and extracted their associated MTR and terrain values from the rasters. Models based on boosted regression trees were used for statistical modeling. They use a sequence of regression (decision) trees to model a response variable where each successive tree predicts the residuals from the previous tree, thus potentially improving predictive performance (Elith et al., 2008). In particular, we applied Gradient Boosted Models (GBMs), which build an ensemble of shallow and weak successive trees with each tree learning and improving on the previous. All the sampling points of both sectors were pooled given their proximity and the similarity of terrain features, in particular the altitudinal range. When implementing this method, we explored the best combination of hyperparameters by varying them (starting number of trees: 10,000; depth of trees: 1–3; bagging fraction: 0.5–1 to allow stochastic gradient descent; minimum number of observations per terminal node: 5–10; learning rate or shrinkage: 0.001–0.5; family: Gaussian), and cross validation by training on 70% of the dataset and using remaining 30% to evaluate performance. The best combination of hyperparameters that resulted in the

model with the lowest RMSE was then used to run the final model. We used the "gbm" package (Greenwell et al., 2022) for R environment for this analysis, and the "relative.influence" function to estimate in % the relative contribution of the eight environmental factors, visualized as partial dependence plots.

3. Results

3.1. Validation of UAV-LST data

The UAV-LST temperatures correlated well with temperatures recorded by the iButtons below ground: coefficients of determination ranged between 0.77 and 0.90. RMSE ranged between 4.91 °C and 7.64 °C. The overall r^2 of temperatures in the four campaigns and sites was 0.81 with RMSE of 5.60 °C. By study sectors, best performances ($r^2 \geq 0.85$) were achieved in O2 (RMSE = 4.91 °C), P3 (RMSE = 5.71 °C), and P2 (RMSE = 5.27 °C) (Fig. 2), but all sectors reached correlation values higher than 0.78. There were also good correlations in minimum temperatures ($r^2 = 0.87$, RMSE = 5.50 °C; Fig. 3) and forests ($r^2 = 0.82$, RMSE = 4.60 °C; Fig. 4), while the lowest correlation value was achieved in maximum temperatures ($r^2 = 0.77$, RMSE = 5.70 °C; Fig. 3). Regarding the validation with the TMS triple-sensor devices, although one sensor in forest failed, we found higher correlations regardless of whether they were in open-air or in forest (Fig. 5), only slightly lower when the sensor was below ground (r2 = 0.90, RMSE = 10.71 °C) and on the ground ($r^2 = 0.90$, RMSE = 3.16 °C) than above ground ($r^2 = 0.92$, RMSE = 1.56 °C). As expected, UAV at canopy level and TMS dataloggers at ground level recorded lower temperatures in forest than in open areas (Fig. 6), being the temperature inside the forest 7.15 °C lower than outside estimated with the UAV, and 10.49 °C, 11.84 °C and 5.54 °C lower estimated by TMS dataloggers (below, on, and above ground, respectively).

3.2. Spatial distribution of the most thermally stable sites

The classification into deciles of the frequency distribution of the Daily Thermal Range (DTR) and the Mean Thermal Range (MTR) allowed us to clearly distinguish areas thermally stable in the six study sectors. They were mainly found in three locations: the north-facing slopes, small sites under the shade of rocky cliffs, and forests regardless of aspect. DTRs showed that these three locations were always within the D1 and D2 (very-high and high thermal stability, respectively; see also Figs. S2 and S3 of Supplementary Materials). Most of the areas in northern slopes showed thermal stability, with patches of very-high thermal stability, as observed in O1, O3, and the three sectors of the Pineta Valley, with varying spatial extents that were minimum in summer and maximum in autumn. Small sites under rocky cliffs in O1 and O3 were always thermally very stable (D1) in all seasons, and only for autumn in O3 the rank descended to D2. Forested areas were always within the D1 and were located not only on shady slopes, but also on sunny slopes (e.g., areas O2, P1, P2, and P3). MTRs, resulting from combining DTRs across seasons (Fig. 7), showed that most of the sites of these three locations were within the D1 of very-high thermal stability, hence they could be considered as microrefugia. On the contrary, the locations of higher thermal ranges corresponded to grasslands in plains and south-facing slopes, and the large north-facing nude scree of P3, which is the site with largest thermal range of the entire north slope of *Sierra de Espierba* sector.

3.3. Variables promoting microrefugia

Boosted regression models returned a minimum RMSE of 2.74. Northness was the most influential predictor (37.39%), increasing thermal stability (i.e., low MTR) as soon as the area was slightly oriented towards north (Fig. 8). The slope was the second most important predictor (16.65%), promoting thermal stability in areas with slopes from

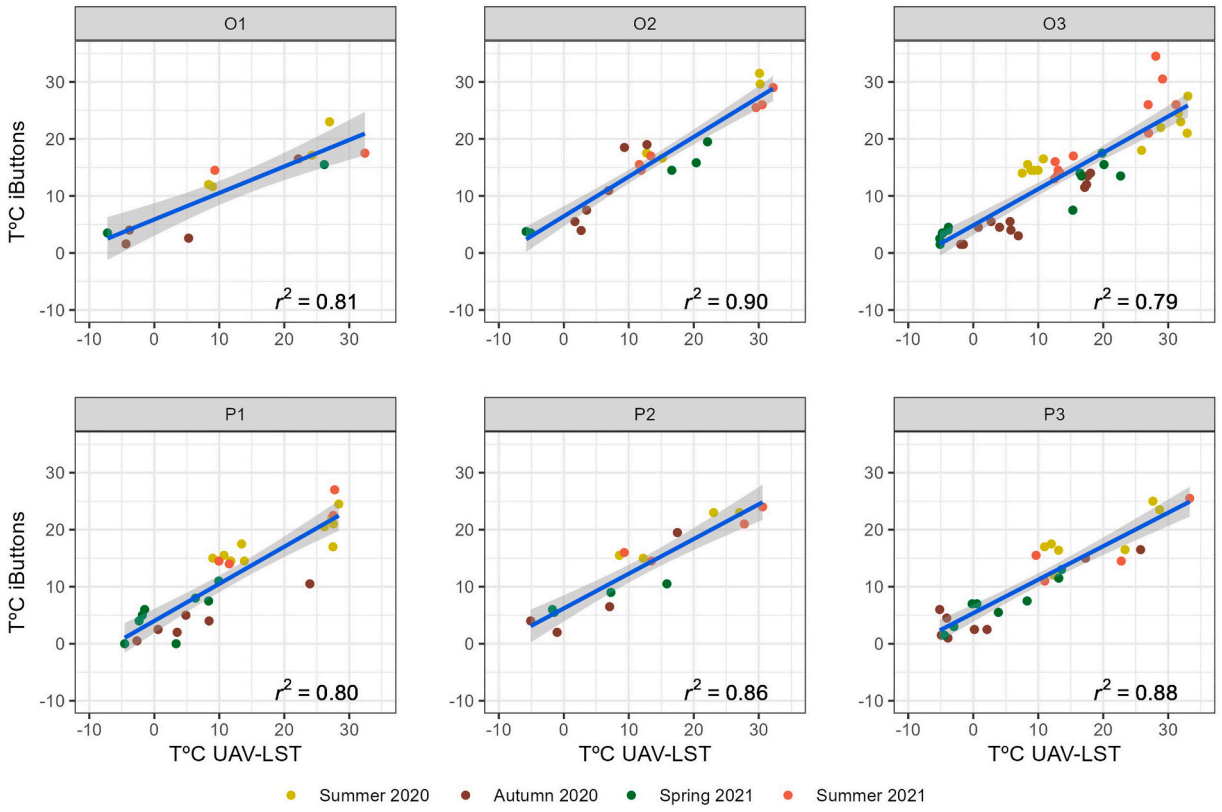

Fig. 2. Relationship between temperatures measured by *iButtons* and estimated by the UAV in the same *iButton* location for each study sector. All coefficients had a *p*-value <0.05.

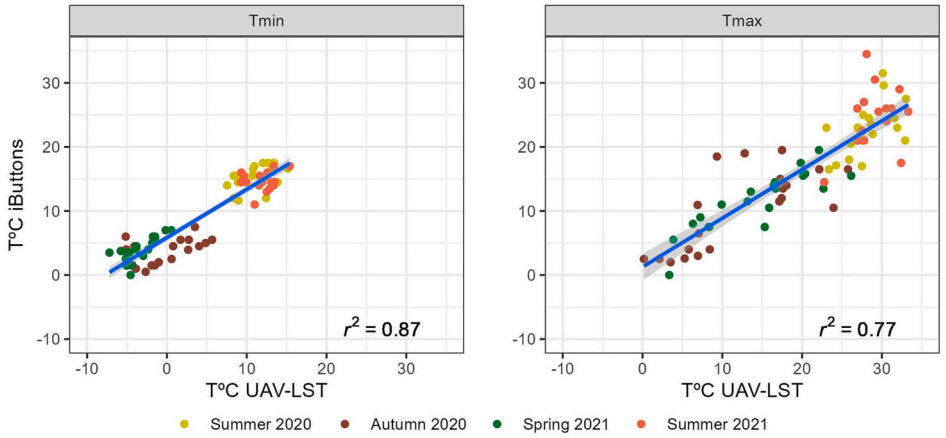

Fig. 3. Relationship between minimum (Tmin) and maximum (Tmax) temperatures measured by *iButtons* and estimated by the UAV in the same *iButton* location. All coefficients had a p-value <0.05.

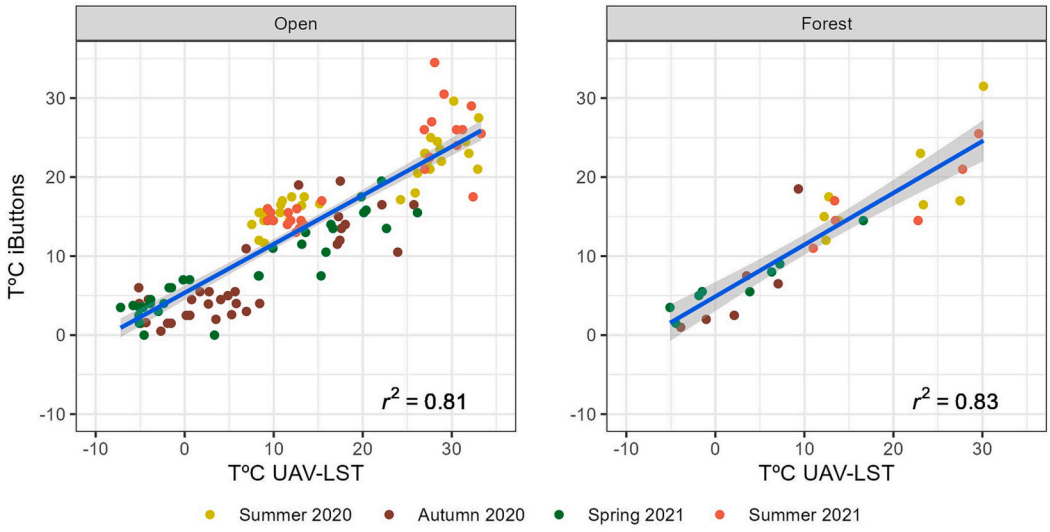

Fig. 4. Relationship between open-air and forested temperatures measured by *iButtons* and estimated by the UAV in the same *iButton* location. All coefficients had a p-value <0.05.

35°-40°, such as rocky cliffs, also because north-oriented slopes tend to be steeper than south-oriented slopes in the study area. Forest density was the third relevant predictor (13.80%), and the partial dependence plot shows that the MTR decreases as forest density increases, indicating its strong effect in promoting thermal stability. MTR increases with WEI (11.04%), meaning that the sites less exposed to the wind experience more thermal stability. The heat load (7.85%) decreased thermal stability, so sites less exposed to incoming solar radiation were more stable. The rest of the variables had <5% of relative importance in promoting thermal stability: Eastness (4.82%) dramatically shifts MTR between east and west aspects; SWI (4.24%) indicates less thermal stability in areas of great run-off generation potential; and VRM (4.21%) promote stability when ruggedness is very high.

4. Discussion

In the current context of climate change, developing actions to mitigate the detrimental effect of warming on biodiversity is of high priority. However, a very simple and first step to be effective would be to identify microrefugia and the species they shelter, which would benefit from long-term thermal stability and lower exposition to extreme climatic effects (Ashcroft et al., 2012; Dobrowski, 2011; Keppel et al., 2015). This study has developed a novel methodological approach to tackle such challenge in topographically complex areas, consisting in the use of a thermal UAV for the detection of very-high thermally stable areas at centimetric scale. Nonetheless, our method can be easily extrapolated to other non-mountainous areas with potential conditions for the presence of microrefugia, such as flatter areas with micro-topography, wetlands, or patches of woody vegetation. Our method also overcomes the limitations of other remote sensing platforms, such as manual thermo-cameras, which are limited in terms of mobility, or spaceborne sensors, whose spatial resolution does not allow the identification of microclimates and, therefore, microrefugia. It is interesting to discover the improvement achieved by the UAV with respect to the commonly used MODIS images: Fig. 9 shows the range of temperatures of each UAV thermal image and the single MODIS LST value returned from the satellite of the same day at almost the same time in the three flying areas of Pineta sector (Aug 1, 2020; MODIS time: 8:30 UTC; UAV time: 6–8 UTC; "MOD11A1 v6" product: https://lpdaac.usgs.gov/products/mod11a1v006/, accessed 30 May 2022).

4.1. UAV accuracy for estimating land surface temperatures

To accurately identify areas with low thermal ranges, an essential

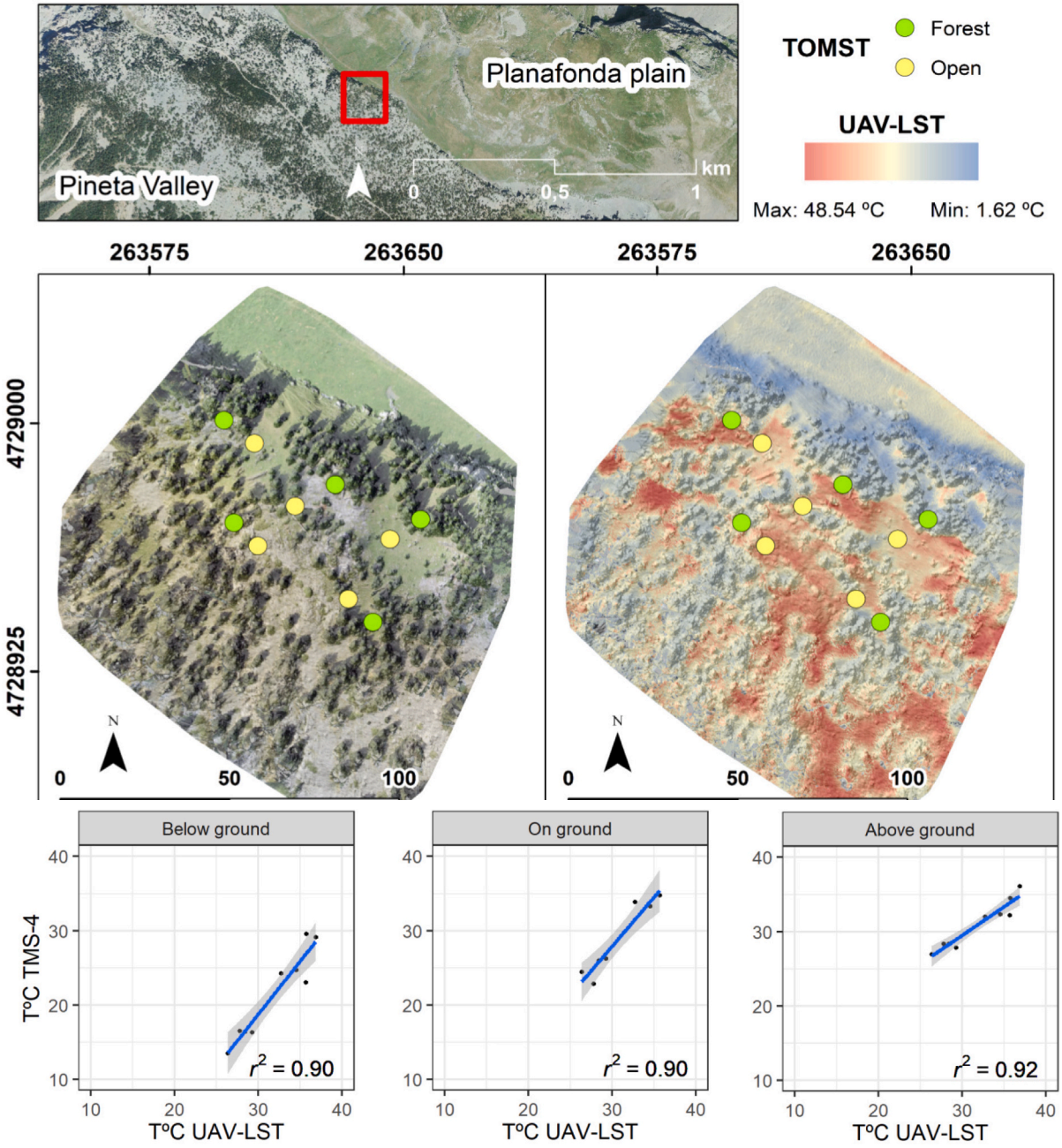

Fig. 5. Spatial distribution of the TMS dataloggers (above) over RGB (left) and TIR (right) imageries and relationship between temperatures measured by the TMS dataloggers and estimated by the UAV in the same TMS location (below). All coefficients had a p-value <0.05.

first step is to validate land surface temperatures (LST) estimated by the UAV. For this end, we confronted UAV-LST data with temperature records of a net of miniaturized field sensors, which were well considered as validation tools because of their good accuracy in estimating temperatures when not exposed directly to solar radiation (see Hubbart et al., 2005; Wild et al., 2019). The importance of this validation also lies in the fact that the TIR region is affected by the emissivity of the different surface materials, which usually ranges between 0.88 and 0.99 (Messina and Modica, 2020). However, in this study a default emissivity of 0.95 was set to all UAV flights due to the very-high resolution images and the highly varied individual surface types (Coutts et al., 2016). Correlation between UAV-LST and field sensor records yielded very good overall coefficients, even considering that iButtons were deployed at about 5 cm below ground, where thermal conditions tend to be less extreme than on ground level (Zellweger et al., 2020; Hoffrén et al., 2022), from which LST records came from. In fact, the adjustment between UAV-LST data and the 'below ground' and 'on ground' temperatures given by the TMS loggers were very similar, slightly better for the sensor above the ground. There is still room for improvement in the good correlation we found between UAV-LST data and iButtons and TMS estimates. On the one hand, it was carried out by averaging pixels in circular buffers due to the uncertainty in the loggers position, which can be shorten in future studies using differential GPS. On the other hand, we have worked with a low-resolution TIR sensor, but temperature data has been obtained at a very high spatial resolution. Although RMSE values were high when comparing the UAV temperatures with the iButtons and TMS loggers below ground, they were lower with the TMS on and above ground, the layer where UAVs record temperatures. More accurate results could be

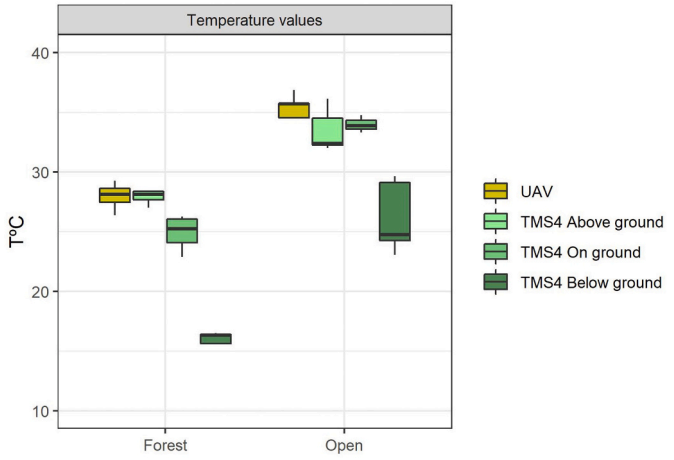

Fig. 6. Temperatures in forest and open areas recorded by UAV and TMS dataloggers in the Pineta sunny slope.

obtained by the use of UAVs with higher resolution TIR sensors, as well as by the improvement of UAV technology in the future, but our results support the idea that thermal UAVs can be reliable tools for identifying microclimates and thus for finding out potential microrefugia of high thermal stability.

4.2. *Where do microrefugia tend to locate?*

In this study, our thermal UAV has been able to identify small to medium scattered areas of high and very-high thermal stability at sub-alpine level (~2100 m a.s.l.), which followed some common spatial patterns in the six study sectors. Thermally stable areas were frequently located on northern slopes, being the northness the terrain variable of highest influence for the occurrence of potential microrefugia of thermal stability. These results are to be expected, as northern slopes of mountains of the northern hemisphere are subject to less extreme maximum temperatures because of the greater sun rays angle of incidence, resulting in narrower thermal ranges and cooler environments (see Rita et al., 2021). Consequently, irrespective of their size, areas of north slopes constitute good candidates to become microrefugia for cold-adapted and mesophilic organisms as proposed by Dobrowski (2011).

The second area of very-high thermal stability was found in locations under prominent rocky landforms like north-facing cliffs, especially in O1 and O3. These open areas had always very low thermal range (D1) in almost all seasons except for the autumn in O3 (D2), when the vegetative period is over for many plants. The slope variable, which was the second most significant in the boosted regression model, shows that very steep areas such as cliffs promote thermal stability. Whereas an increase in the thermal range was observed on slopes between 20° and 35° (Fig. 8), a dramatic decrease appears above 35°, which can be explained by the fact that the former are predominantly south-facing whereas the latter are more often north-facing in our study area. In this sense, sites near cliffs located on northern slopes can accentuate protection against solar radiation in summer and cold winds, making temperatures more stable overall, as well as within multiple small crevices they have, that in turn contribute to creating smaller microhabitats.

The third more significant variable promoting very-high thermal stability was forest density, a proxy of canopy forest. As expected, and regardless of aspect, forested areas showed very low thermal ranges in all seasons, so most of them fell within the D1 of very-high thermal stability. We found high correlations between UAV-LST and TMS records in small mixed patches of forest and clearings in the sunny slope of Pineta Valley, which confirmed the cooling effect of trees even at low

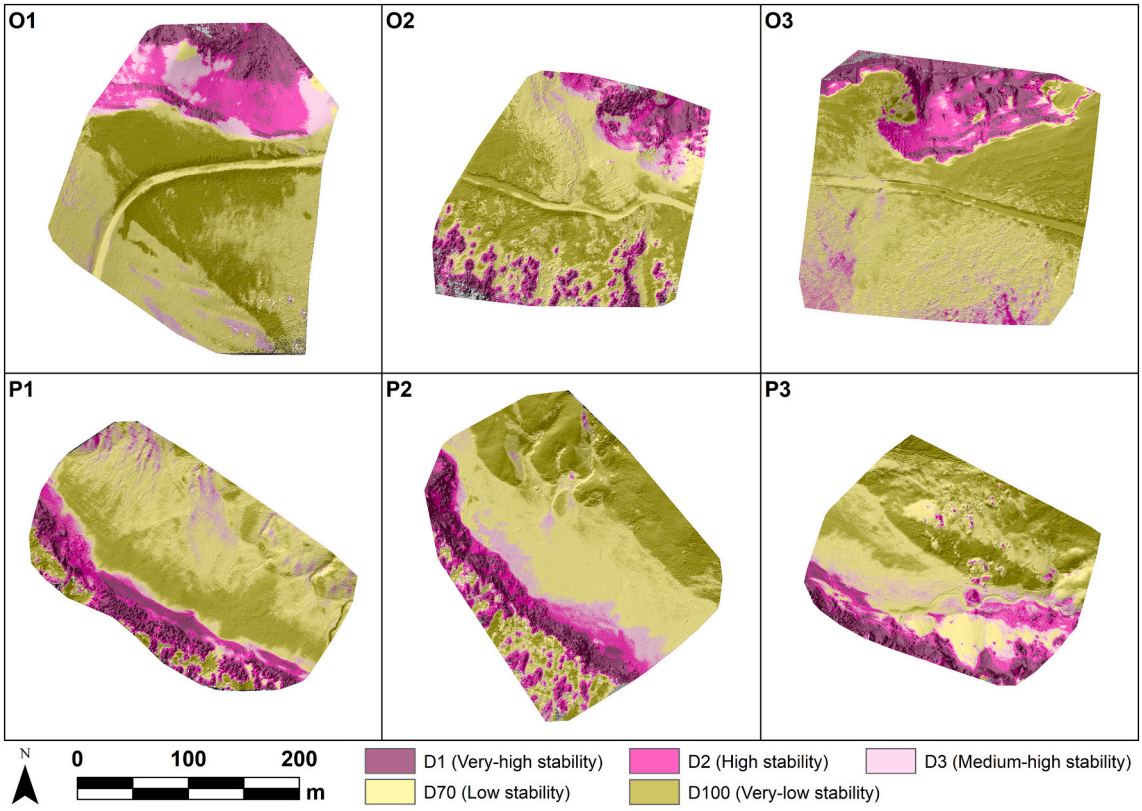

Fig. 7. Locations found with very-high thermal stability (D1, in dark pink), high thermal stability (D2, in pink), and medium-high thermal stability (D3, in light pink) across the six study sectors throughout the seasons with UAV flight (MTR: Mean Thermal Range). (For interpretation of the references to colour in this figure legend, the reader is referred to the web version of this article.)

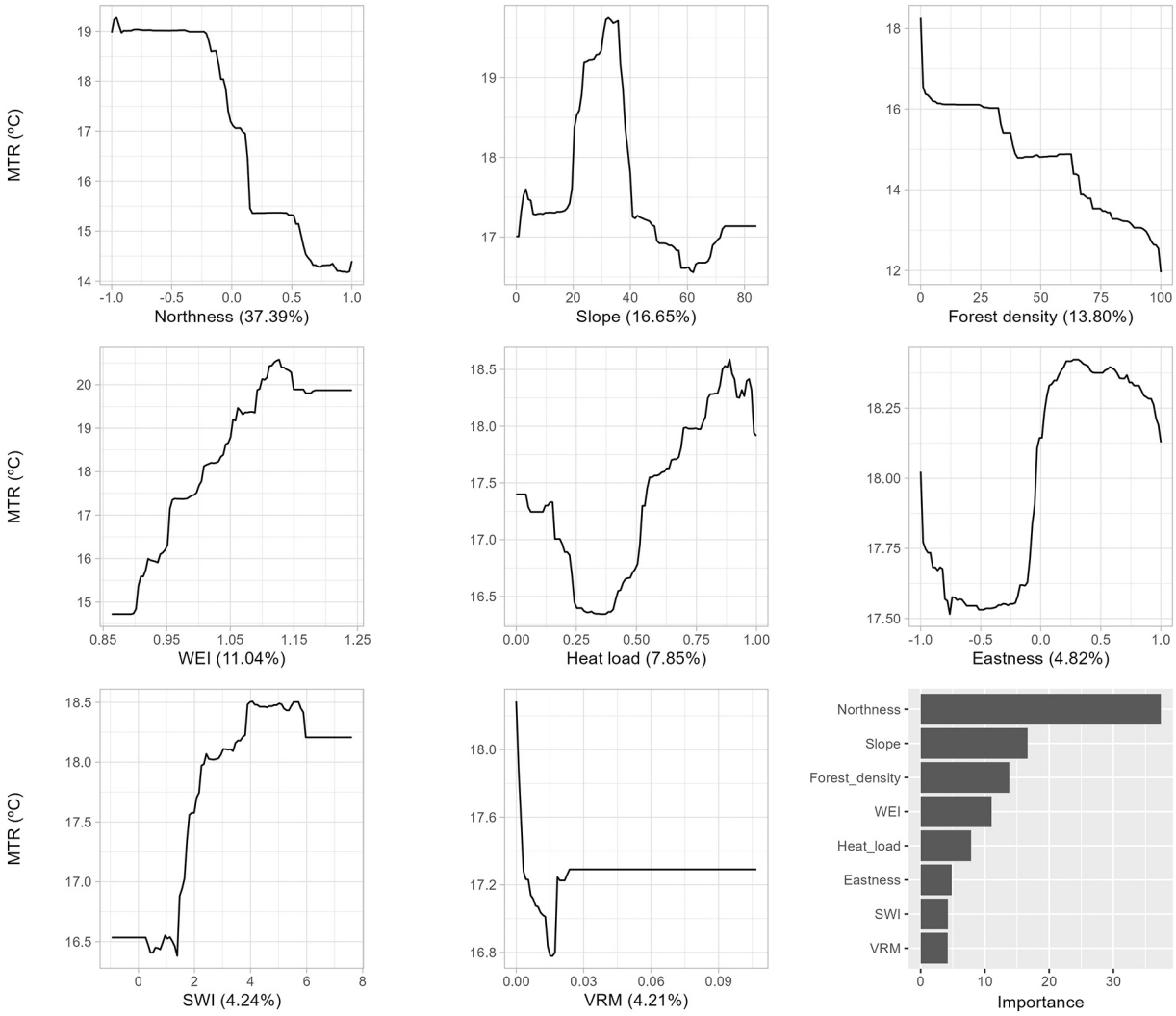

Fig. 8. Partial dependence plots for the predictors of MTR (Mean Thermal Range) used in the boosted regression tree models, arranged in order of relative influence (%).

density, and allow us to conclude that temperatures recorded by the UAV reflect well the thermal conditions below the canopy in low dense forests. The buffering effect of forest on temperatures is well known: tree canopies provide protection to ground-dwelling organisms from extreme conditions of temperature because they hinder the penetration of solar radiation, thus producing lower thermal ranges (De Frenne et al., 2019). Latimer and Zuckerberg (2016) already observed higher thermal ranges in fragmented forests, where cooler minimum and mean daily temperatures were registered than in compact forest areas. In this sense, our UAV has perfectly identified these buffered areas despite canopy density was not very high at such elevation, including those in sunny slopes where thermal ranges are more extreme in general.

In sum: both topographic heterogeneity and the presence of forests have the capacity to create refugia at micro- and mesoscale (cm till hundreds of m^2). The role of rocky habitats (except nude screes in homogenous slopes) acting as potential microrefugia is supported by other studies that demonstrated they harbor abundant endemic and range-bound species (e.g., Bátori et al., 2017; Bátori et al., 2020; García et al., 2020; Schut et al., 2014). It has been shown that north aspects and rocky habitats have been the key to the persistence of biodiversity during the last glacial period (Bennett et al., 1991; Bennett and Provan, 2008; Birks and Willis, 2008; Dobrowski, 2011; Keppel et al., 2011), allowing ancient plant lineages to persist under adverse environmental conditions. Topographic variation has recently been proposed as one of the main factors halting the extinction of populations of plants and insects (Suggitt et al., 2018), and cold rocky landforms in particular as key climate refugia for terrestrial and aquatic biodiversity in mountain ecosystems (Brighenti et al., 2021). Concerning forests, the mechanistic process and the remarkable beneficial effect of canopies in buffering extreme temperatures has also largely been documented (e.g., De Frenne et al., 2019). The buffering effect of forests has been proposed as crucial for the persistence of species occurring under their canopy both at ecological and evolutionary scale (García et al., 2022). Interestingly, an important but often forgotten detail is that forests can be transformed and, unlike forests, rocky habitats such as cliffs remain even under strong land use changes, so that these areas have a high long-term ecosystem value.

5. Conclusions

Identification of small areas with stable temperatures is a priority first step for the detection of microrefugia for biodiversity conservation in the current context of climate change. In this sense, UAVs offer an unprecedented chance for the detection of microclimates and microrefugia in mountain regions at very-high spatial resolution, impossible to achieve through airborne or spaceborne sensors. Our results conclude that thermal UAVs are capable of detecting areas of high thermal stability throughout a year, a key feature of microrefugia. In our study

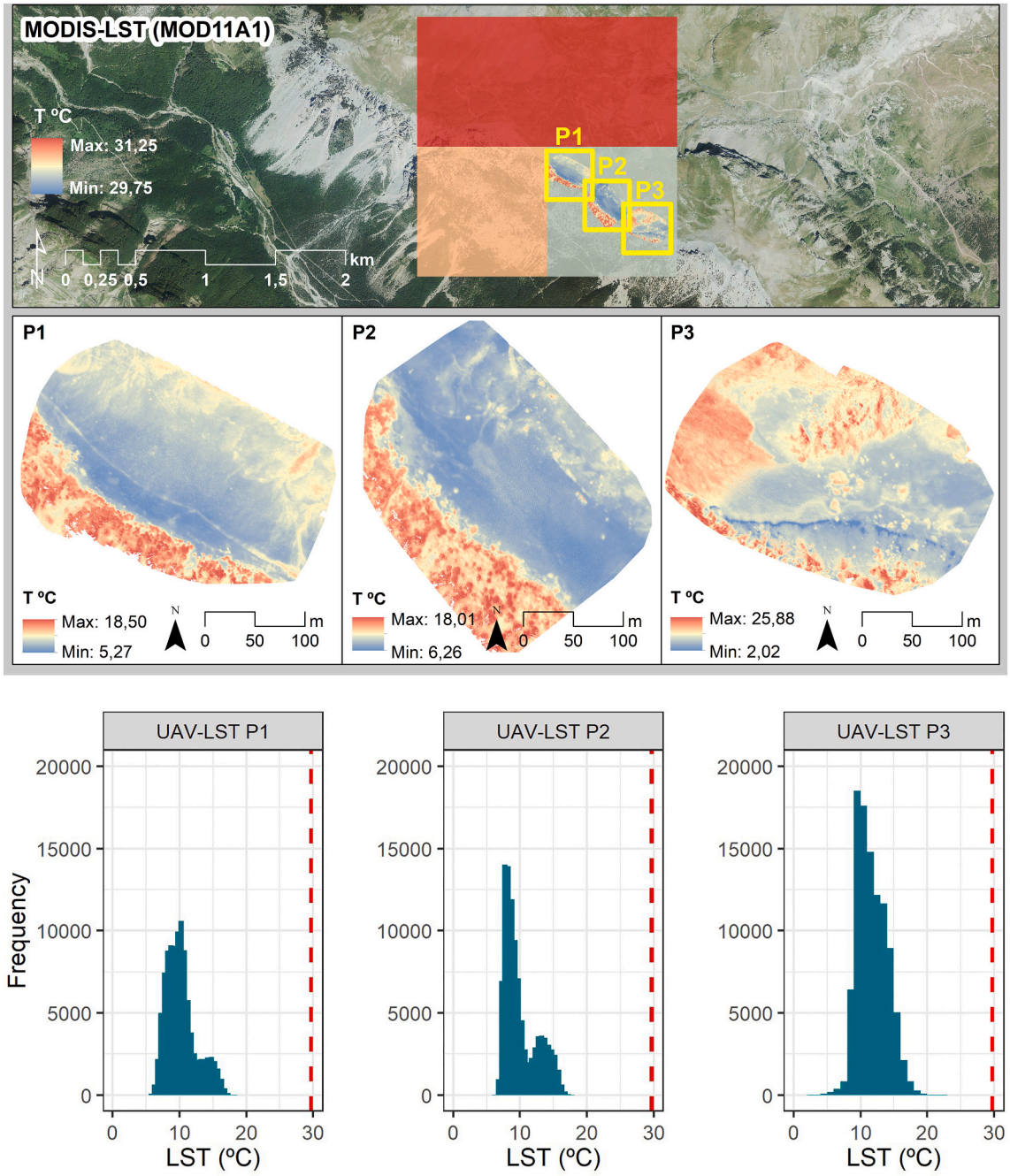

Fig. 9. Comparison of temperatures provided by satellite and UAV devices in the three Pineta sectors. Above: MODIS LST pixels (MOD11A1) returning a single temperature, and UAV-LST thermal landscapes of P1, P2, and P3. Overlapped areas show the microclimatic heterogeneity within MODIS pixels. Below: Frequency distribution of the UAV-LST data pixels of the three areas of Pineta sector (P1, P2, and P3) and the MODIS LST pixel value within the three areas (red dashed line). (For interpretation of the references to colour in this figure legend, the reader is referred to the web version of this article.)

region, we easily associated those areas to northern slopes, small sites under rocky cliffs, and forested areas. Further research will be needed in the future to better understand the capabilities and limitations of these promising instruments, but our results shed light on its utility to accurately identify microrefugia, and thereby to successfully contribute to prevent biodiversity loss.

Credit author statement

R.H. and M.B.G. conceptualized the study, acquired and processed the field data, implemented the statistical analyses, and wrote the original manuscript. R.H. carried out the UAV flights, and processed and analyzed the UAV data.

Funding

This work was supported by the Spanish Association of Terrestrial Ecology (AEET) through the program "Grants for research projects led by young researchers 2019"; the Spanish Ministry of Science, Innovation, and Universities through an FPU predoctoral contract granted to R. H. (FPU18/05027); and the Spanish Research Agency through the VULBIMON (CGL2017-90040-R) and REFUGIA (PID2021-129056OB-

I00) projects to M.B.G.

CRediT authorship contribution statement

R. Hoffrén: Conceptualization, Methodology, Validation, Formal analysis, Resources, Writing – original draft, Writing – review & editing, Software, Data curation. **M.B. García:** Conceptualization, Methodology, Validation, Formal analysis, Resources, Writing – original draft, Writing – review & editing.

Declaration of Competing Interest

The authors declare that they have no known competing financial interests or personal relationships that could have appeared to influence the work reported in this paper.

Data availability

Data will be made available on request.

Acknowledgments

We deeply thank the PNOMP staff, and the Department of Agriculture and Environment of the Government of Aragon, for the permissions to UAV overflights in the protected area and the use of facilities during the study period. We also thank the PNOMP rangers, especially F. Villaespesa, C. Benedé, R. Jiménez, and M. Moreno for their assistance during the UAV flights and access to restricted areas. We thank the town councils of Torla, Fanlo and Bielsa, for the permissions to transit over the restricted roads of Sierra de las Cutas and Sierra de Espierba, and H. Miranda and M. Quintana (IPE-CSIC) for their help in deploying the iButtons. Finally, we would like to thank the two anonymous reviewers for their efforts in improving the manuscript.

Appendix A. Supplementary data

Supplementary data to this article can be found online at https://doi.org/10.1016/j.rse.2022.113427.

References

Ackerly, D.D., Loarie, S.R., Conrwell, W.K., Weiss, S.B., Hamilton, H., Branciforte, R., Kraft, N.J.B., 2010. The geography of climate change: implications for conservation biogeography. Drivers Distrib. 16, 476–487. https://doi.org/10.1111/j.1472-4642.2010.00654.x.

Andrew, M.E., Warrener, H., 2017. Detecting microrefugia in semi-arid landscapes from remotely sensed vegetation dynamics. Remote Sens. Environ. 200, 114–124. https://doi.org/10.1016/j.rse.2017.08.005.

Ashcroft, M.B., Gollan, J.R., 2013. Moisture, thermal inertial, and the spatial distributions of near-surface soil and air temperatures: understanding factors that promote microrefugia. Agr. & Forest Meteo. 176, 77–89.

Ashcroft, M.B., Chisholm, L.A., French, K.O., 2009. Climate change at the landscape scale: predicting fine-grained spatial heterogeneity in warming and potential refugia for vegetation. Glob. Chang. Biol. 15 (3), 656–667. https://doi.org/10.1111/j.1365-2486.2008.01762.x.

Ashcroft, M.B., Gollan, J.R., Warton, D.I., Ramp, D., 2012. A novel approach to quantify and locate potential microrefugia using topoclimate, climate stability, and isolation from the matrix. Glob. Chang. Biol. 18, 1866–1879. https://doi.org/10.1111/j.1365-2486.2012.02661.x.

Bátori, Z., Vojtkó, A., Farkas, T., Szabó, A., Havadtöi, K., Vojtkó, A.E., Tölgyesi, C., Cseh, V., Erdös, L., Maák, I.E., Keppel, G., 2017. Large- and small-scale environmental factors drive distributions of cool-adapted plants in karstic microrefugia. Ann. Bot. 119, 301–309. https://doi.org/10.1093/aob/mcw233.

Bátori, Z., Lörinczi, G., Tölgyesi, C., Módra, G., Juhász, O., Aguilón, D.J., Vojtkó, A., Valkó, O., Deák, B., Erdös, L., Maák, I.E., 2020. Karstic microrefugia host functionally specific ant assemblages. Front. Ecol. Evol. 23 (8) https://doi.org/10.3389/fevo.2020.613738.

Bennett, K.D., Provan, J., 2008. What do we mean by 'refugia'? Quat. Sci. Rev. 27 (27–28), 2449–2455. https://doi.org/10.1016/j.quascirev.2008.08.019.

Bennett, K.D., Tzedakis, P.C., Willis, K.J., 1991. Quaternary refugia of North European trees. J. Biog. 18 (1), 103–115. https://doi.org/10.2307/2845248.

Beven, K.J., Kirkby, M.J., 1979. A physically based, variable contributing area model of basin hydrology / Un modèle à base physique de zone d'appel variable de l'hydrologie du basin versant. Hydrol. Sci. J. 24 (1), 43–69. https://doi.org/10.1080/02626667909491834.

Birks, H.J.B., Willis, K.J., 2008. Alpines, trees, and refugia in Europe. Plant Ecol. Divers. 1, 147–160. https://doi.org/10.1080/17550870802349146.

Böhner, J., Selige, T., 2006. Spatial prediction of soil attributes using terrain analysis and climate regionalization. In: Böhner, J., McCloy, K.R., Strobl, J. (Eds.), SAGA – Analysis and Modelling Applications. Göttinger Geographische Abhaundlungen, Göttingen, pp. 13–28.

Böhner, J., Koethe, R., Conrad, O., Gross, J., Ringeler, A., Selige, T., 2002. Soil regionalisation by means of terrain analysis and process parameterization. In: Micheli, E., Nachtergaele, F., Montanarella, L. (Eds.), Soil Classification 2001. European Soil Bureau, Research Report No. 7, EUR 20398 EN, Luxembourg, pp. 213–222.

Brighenti, S., Hotaling, S., Finn, D.S., Fountain, A.G., Hayashi, M., Herbst, D., Saros, J.E., Tronstad, L.M., Millar, C.I., 2021. Rock glaciers and related cold rocky landforms: overlooked climate refugia for mountain biodiversity. Glob. Chang. Biol. 27, 1504–1517. https://doi.org/10.1111/gcb.15510.

Chen, I.C., Hill, J.K., Ohlemüller, R., Roy, D.B., Thomas, C.D., 2011. Rapid range shifts of species associated with high levels of climate warming. Science 333, 1024–1026.

Choler, P., 2017. Winter soil temperature dependence of alpine plant distribution: implications for anticipating vegetation changes under a warming climate. Persp. Plant Ecol. Evol. Syst. 30, 6–15. https://doi.org/10.1016/j.ppees.2017.11.002.

Collins, A.F., Bush, M.B., Sachs, J.P., 2013. Microrefugia and species persistence in the Galápagos highlands: a 26,000-year paleoecological perspective. Front. Genet. 4, 269. https://doi.org/10.3389/fgene.2013.00269.

Conrad, O., Bechtel, B., Bock, M., Dietrich, H., Fischer, E., Gerlitz, L., Wehberg, J., Wichmann, V., Böhner, J., 2015. System for automated geoscientific analyses (SAGA) v. 2.1.4. Geosci. Model Dev. 8, 1991–2007. https://doi.org/10.5194/gmd-8-1991-2015.

Coutts, A.M., Harris, R.J., Phan, T., Livesley, S.J., Williams, N.S.G., Tapper, N.J., 2016. Thermal infrared remote sensing of urban heat: hotspots, vegetation, and an assessment of techniques for use in urban planning. Remote Sens. Environ. 186, 637–651. https://doi.org/10.1016/j.rse.2016.09.007.

Davis, F.W., Flint, A.L., Fricker, G.A., McCullough, I.M., Franklin, J., Serra-Díaz, J.M., Synes, N.W., 2019. LiDAR-derived topography and forest structure predict fine-scale variation in daily surface temperatures in oak savanna and conifer forest landscapes. UC Riverside. https://doi.org/10.1016/j.agrformet.2019.02.015.

De Frenne, P., Zellweger, F., Rodríguez-Sánchez, F., Scheffers, B.R., Hylander, K., Luoto, M., Vellend, M., Verheyen, K., Lenoir, J., 2019. Global buffering of temperatures under forest canopies. Nat. Ecol. Evol. 3, 744–749. https://doi.org/10.1038/s41559-019-0842-1.

De Frenne, P., Lenoir, J., Luoto, M., Scheffers, B.R., Zellweger, F., Aalto, J., Ashcroft, M. B., Christiansen, D.M., Decocq, G., De Pauw, K., Govaert, S., Greiser, C., Gril, E., Hampe, A., Jucker, T., Klinges, D.H., Koelemeijer, I.A., Lembrechts, J.J., Marrec, R., Meeussen, C., Ogée, J., Tyystjärvi, V., Vangansbeke, P., Hylander, K., 2021. Forest microclimates and climate change: importance, drivers and future research agenda. Glob. Chang. Biol. 27, 2279–2297. https://doi.org/10.1111/gcb.15569.

Dobrowski, S.Z., 2011. A climatic basis for microrefugia: the influence of terrain on climate. Glob. Chang. Biol. 17, 1022–1035. https://doi.org/10.1111/j.1365-2486.2010.02263.x.

Elith, J., Leathwick, J.R., Hastle, T., 2008. A working guide to boosted regression trees. J. Anim. Ecol. 77, 802–813. https://doi.org/10.1111/j1365-2656.2008.01390.x.

Evans, J.S., Hudak, A.T., 2007. A multiscale curvature algorithm for classifying discrete return LiDAR in forested environments. IEEE Trans. Geosci. Remote 45, 1029–1038. https://doi.org/10.1109/TGRS.2006.890412.

Faye, E., Rebaudo, F., Yánez-Cajo, D., Cauvy-Fraunié, S., Dangles, O., 2016. A toolbox for studying thermal heterogeneity across spatial scales: from unmanned aerial vehicle imagery to landscapes metrics. Methods Ecol. Evol. 7 (4), 437–446. https://doi.org/10.1111/2041-210X.12488.

García, M.B., Domingo, D., Pizarro, M., Font, X., Gómez, D., Ehrlén, J., 2020. Rocky habitats as microclimatic refuges for biodiversity: a close-up thermal approach. Environ. Exp. Bot. 170, 103886 https://doi.org/10.1016/j.envexpbot.2019.103886.

García, M.B., Miranda, H., Pizarro, M., Font, X., Roquet, P., González-Sampériz, P., 2022. Habitats hold a phylogenetic signal of past climatic refugia. Biodivers. Conserv. https://doi.org/10.1007/s10531-022-02419-4.

Graae, B.J., Vandvik, V., Ambruster, W.S., Eiserhardt, W.L., Svenning, J.C., Hylander, K., Ehrlén, J., Speed, J.D.M., Klanderud, K., Brathen, K.A., Milbau, A., Opedal, O.H., Alsos, I.G., Ejrnaes, R., Bruun, H.H., Birks, H.J.B., Westergaard, K.B., Birks, H.H., Lenoir, J., 2018. Stay or go: how topographic complexity influences alpine plant population and community responses to climate change. Persp. Plant Ecol., Evol. & Syst. 30, 41–50. https://doi.org/10.1016/j.ppees.2017.09.008.

Greenwell, B., Boehmke, B., Cunningham, J., Developers, G., 2022. gbm. Generalized Boosted Regression Models. R Package Version 2.1.8.1. Available online: https://CRAN.R-project.org/package=gbm (accessed 13 Dec 2022).

Greiser, C., Meineri, E., Luoto, M., Ehrlén, J., Hylander, K., 2018. Monthly microclimate models in a managed boreal forest landscape. Agr. Forest Meteo. 250-251, 147–158. https://doi.org/10.1016/j.agrformet.2017.12.252.

Greiser, C., Ehrlén, J., Meineri, E., Hylander, K., 2019. Hiding from the climate: characterizing microrefugia for boreal forest understory species. Glob. Chang. Biol. 26 (2), 471–483. https://doi.org/10.1111/gcb.14874.

Hedley, C.B., Roudier, P., Yule, I.J., Ekanayake, J., Bradbury, S., 2013. Soil water status and water table depth modelling using electromagnetic surveys for precision irrigation scheduling. Geoderma 199, 22–29. https://doi.org/10.1016/j.geoderma.2012.07.018.

Hijmans, R.J., 2021. raster. Geographic data analysis and modeling. R Package Version 3.1-13. Available online: https://CRAN.R-project.org/package=raster.

Hoffrén, R., Miranda, H., Pizarro, M., Tejero, P., García, M.B., 2022. Identifying the factors behind climate diversification and refugial capacity in mountain landscapes: the key role of forests. Remote Sens. 14, 1708. https://doi.org/10.3390/rs14071708.

Hubbart, J.A., Link, T.E., Campbell, C., Cobos, D., 2005. Evaluation of a low-cost temperature measurement system for environmental applications. Hydrol. Process. 19 (7), 1517–1523. https://doi.org/10.1002/hyp.5861.

Hylander, K., Ehrlén, J., Luoto, M., Meineri, E., 2015. Microrefugia: not for everyone. AMBIO 44, 60–68. https://doi.org/10.1007/s13280-014-0599-3.

Keppel, G., van Niel, K.O., Wardell-Johnson, G.W., Yates, C.J., Byrne, M., Mucina, L., Schut, A.G.T., Hopper, S.D., Franklin, S.E., 2011. Refugia: identifying and understanding safe havens for biodiversity under climate change. Glob. Ecol. Biogeogr. 21 (4), 393–404. https://doi.org/10.1111/j.1466-8238.2011.00686.x.

Keppel, G., Mokany, K., Wardell-Johnson, G.W., Phillips, B.L., Welbergen, J.A., Reside, A.E., 2015. The capacity of refugia for conservation planning under climate change. Front. Ecol. Environ. 13 (2), 106–112. https://doi.org/10.1890/140055.

Keppel, G., Robinson, T.P., Wardell-Johnson, G.W., Yates, C.J., van Niel, K.P., Byrne, M., Schut, A.G.T., 2017. A low-altitude mountain range as an important refugium for two narrow endemeics in the Southwest Australian Floristic Region biodiversity hotspot. Ann. Bot. 119 (2), 289–300. https://doi.org/10.1093/aob/mcw182.

Körner, C., 2004. Mountain biodiversity, its causes and function. AMBIO Spec 13, 11–17.

Latimer, C.E., Zuckerberg, B., 2016. Forest fragmentation alters winter microclimates and microrefugia in human-modified landscapes. Ecog. 40 (1), 158–170. https://doi.org/10.5061/dryad.rk398.

Lembrechts, J.J., Aalto, J., Ashcroft, M.B., et al., 2020. SoilTemp: a global database of near-surface temperature. Glob. Chang. Biol. 26, 6616–6629. https://doi.org/10.1111/gcb.15123.

Macek, M., Kopecký, M., Wild, J., 2019. Maximum air temperature controlled by landscape topography affects plant species topography in temperate forests. Landsc. Ecol. 34, 2541–2556. https://doi.org/10.1007/s10980-019-00903-x.

Mackey, B., Berry, S., High, S., Ferrier, S., Harwood, T.D., Williams, K.J., 2012. Ecosystem greenspots: identifying potential drought, fire, and climate changes micro-refuges. Ecol. Appl. 22 (6), 1852–1864. https://doi.org/10.1890/11-1479.1.

Maclean, I.M.D., Suggitt, A.J., Wilson, R.J., Duffy, J.P., Bennie, J.J., 2016. Fine-scale climate change: modelling spatial variation in biologically meaningful rates of warming. Glob. Chang. Biol. 23 (1), 256–268. https://doi.org/10.1111/gcb.13343.

Meineri, E., Hylander, K., 2016. Fine-grain, large-domain climate models based on climate stations and comprehensive topographic information improve microrefugia detection. Ecog. 40, 1003–1013. https://doi.org/10.1111/ecog.02494.

Messina, G., Modica, G., 2020. Applications of UAV thermal imagery in precision agriculture: state of the art and future research outlook. Remote Sens. 12, 1491. https://doi.org/10.3390/rs12091491.

Messinger, M., Asner, G., Silman, M., 2016. Rapid assessments of Amazon forest structure and biomass using small unmanned aerial systems. Remote Sens. 8, 615. https://doi.org/10.3390/rs8080615.

Milling, C.R., Rachlow, J.L., Olsoy, P.J., Chappell, M.A., Johnson, T.R., Forbey, J.S., Shipley, L.A., Thornton, D.H., 2018. Habitat structure modifies microclimate: an approach for mapping fine-scale thermal refuge. Methods Ecol. Evol. 9 (6), 1648–1657. https://doi.org/10.1111/2041-210X.13008.

Montealegre, A.L., Lamelas, M.T., de la Riva, J., 2015. A comparison of open-source LiDAR filtering algorithms in a Mediterranean forest environment. IEEE J. Sel Top. Appl. Earth Obs. Remote Sens. 8 (8), 4072–4085. https://doi.org/10.1109/JSTARS.2015.2436974.

Niskanen, A., Luoto, M., Väre, H., Heikkinen, R.K., 2017. Models of arctic-alpine refugia highlight importance of climate and local topography. Polar Biol. 40, 489–502. https://doi.org/10.1007/s00300-016-1973-3.

Olaya, V., Conrad, O., 2009. In: Hengl, T., Reuter, H.I. (Eds.), Geomorphometry in SAGA. Chapter 12 in Geomorphometry Concepts, Software, Applications, Developments in Soil Science, 33. Elsevier, UK. https://doi.org/10.1016/S0166-2481(08)00012-3, 765 pp.

Pardo, I., Roquet, C., Lavergne, S., Olesen, J.M., García, M.B., 2017. Spatial congruence between taxonomic, phylogenetic and functional hotspots: true pattern or methodological artifact? Divers. Distrib. 23, 2029–2220. https://doi.org/10.1111/ddi.12511.

Pauli, H., Gottfried, M., Dullinger, S., Abdaladze, O., Akhalkatsi, M., Benito-Alonso, J.L., Coldea, G., Dick, J., Erschbamer, B., Fernández-Calzado, R., Ghosn, D., Holten, J.I., Kanka, R., Kazakis, G., Kollár, J., Larsson, P., Moiseev, P., Moiseev, D., Molau, U., Molero-Mesa, J., Nagy, L., Pelino, G., Puscas, M., Rossi, G., Stanisci, A., Syverhuset, A.O., Theurillat, J.P., Tomaselli, M., Unterluggauer, P., Villar, L., Vittoz, P., Grabherr, G., 2012. Recent plant diversity changes on Europe's mountain summits. Science 336, 6079. https://doi.org/10.1126/science.1219033.

Piedallu, G., Gégout, J.C., 2005. Effects of forest environment and survey protocol on GPS accuracy. PE&RS 71 (9), 1071–1078. https://doi.org/10.14358/PERS.71.9.1071.

Pugnaire, F.I., Morillo, J.A., Peñuelas, J., Reich, P.B., Bardgett, R.D., Gaxiola, A., Wardle, D.A., van der Putten, W.H., 2019. Climate change effects on plant-soil feedbacks and consequences for biodiversity and functioning of terrestrial ecosystems. Sci. Adv. 5 (11), eaaz1834. https://doi.org/10.1126/sciadv.aaz1834.

Puliti, S., Olerka, H., Gobakken, T., Naesset, E., 2015. Inventory of small forest areas using an unmanned aerial system. Remote Sens. 7, 9632–9654. https://doi.org/10.3390/rs70809632.

Remondino, F., Spera, M.G., Nocerino, E., Menna, F., Nex, F., 2014. State of the art in high density image matching. Photogramm. Rec. 29, 144–166. https://doi.org/10.1111/phor.12063.

Renslow, M., 2013. Manual of Airborne Topographic Lidar. The American Society for Photogrammetry and Remote Sensing, Bethesda, MD. ISBN: 978–1570830976.

Rita, A., Bonamoni, G., Allevato, E., Borghetti, M., Cesarano, G., Magavero, V., Rossi, S., Saulino, L., Zotti, M., Saracino, A., 2021. Topography modulates near-ground microclimate in the Mediterranean Fagus sylvatica treeline. Sci. Rep. 11, 8122. https://doi.org/10.1038/s41598-021-87661-6.

Schut, A.G.T., Wardell-Johnson, G.W., Yates, C.J., Keppel, G., Baran, I., Franklin, S.E., Hooper, S.D., Van Niel, K.P., Mucina, L., Byrne, M., 2014. Rapid characterization of vegetation structure to predict refugia and climate change impacts across a global biodiversity hotspot. PLoS One 9, e82778. https://doi.org/10.1371/journal.pone.0082778.

Suggitt, A.J., Wilson, J.R., Isaac, N.J.B., Beale, C.M., Auffret, A.G., August, T., Bennie, J. J., Crick, H.Q.P., Duffield, S., Fox, R., Hopkins, J.J., Macgregor, N.A., Morecroft, M. D., Walker, K.J., Maclean, I.M.D., 2018. Extinction risk from climate change is reduced by microclimatic buffering. Nat. Clim. Chang. 8, 713–717. https://doi.org/10.1038/s41558-018-0231-9.

Wild, J., Kopecký, M., Macek, M., Sanda, M., Jankovec, J., Haase, T., 2019. Climate at ecologically relevant scales: a new temperature and soil moisture logger for long-term microclimate measurement. Agr. & Forest Meteo. 268, 40–47. https://doi.org/10.1016/j.agrformet.2018.12.018.

Williamson, J., Slade, E.M., Luke, S.H., Swinfield, T., Chung, A.Y.C., Coomes, D.A., Heroin, H., Jucker, T., Lewis, O.T., Vairappan, C.S., Rossiter, S.J., Struebig, M.J., 2021. Riparian buffers act as microclimatic refugia in oil palm landscapes. J. Appl. Ecol. 58, 431–442. https://doi.org/10.1111/1365-2664.13784.

Wilson, O.J., Walters, R.J., Mayle, F.E., Lingner, D.V., Vibrans, A.C., 2019. Cold spot microrefugia hold the key to survival for Brazil's Critically Endangered Araucaria tree. Glob. Chang. Biol. 25 (12), 4339–4351. https://doi.org/10.1111/gcb.14755.

Zellweger, F., de Frenne, P., Lenoir, J., Rocchini, D., Coomes, D., 2019. Advances in microclimate ecology arising from remote sensing. Trends Ecol. Evol. 34 (4), 327–341. https://doi.org/10.1016/j.tree.2018.12.012.

Zellweger, F., de Frenne, P., Lenoir, J., Vangansbeke, P., Verheyen, K., Bernhardt-Römermann, M., Coomes, D., et al., 2020. Forest microclimate dynamics drive plant responses to warming. Science 368 (6492), 772–775. https://doi.org/10.1126/science.aba6880.